



ELSEVIER

Chemical Engineering Journal 71 (1998) 207–212

---

---

**Chemical  
Engineering  
Journal**

---

---

## The characteristics of a heat-recirculating ceramic burner

Masahisa Shinoda<sup>a</sup>, Reika Maihara<sup>b</sup>, Noriyuki Kobayashi<sup>c</sup>,  
Norio Arai<sup>d</sup>, Stuart W. Churchill<sup>e,\*</sup>

<sup>a</sup>Department of Chemical Engineering, Tohoku University, Sendai 980-8579, Japan

<sup>b</sup>Research Center for Advanced Energy Conversion, Nagoya University, Nagoya 464-8603, Japan

<sup>c</sup>Department of Energy Engineering and Science, Nagoya University, Nagoya 464-8603, Japan

<sup>d</sup>Research Center for Advanced Energy Conversion, Nagoya University, Nagoya 464-8603, Japan

<sup>e</sup>Department of Chemical Engineering, University of Pennsylvania, Philadelphia PA 19104-6393, USA

Received 2 April 1997; received in revised form 14 April 1998; accepted 9 May 1998

---

### Abstract

An experimental burner of the heat-recirculating-type was constructed and its thermal characteristics were investigated for methane–air fuel-lean combustion. Temperature distributions of air and burned gas flowing in the passes of the burner were determined by means of both experimental measurements and numerical simulations. Using the fractional heat recirculation rate as a criterion for thermal performance, the optimal design of the burner was examined in terms of a chemical parameter (the equivalence ratio), a fluid–mechanical parameter (the Reynolds number) and two geometrical parameters (the aspect ratio and the number of passes). © 1998 Elsevier Science S.A. All rights reserved.

*Keywords:* Heat recirculating; Thermal performance; Ceramic burner

---

### 1. Introduction

Gaseous mixtures are frequently encountered in industrial processing in which the concentration of unburned fuels or other combustibles is significant but insufficient to support combustion without preheating. One method of preheating is by exchange between the burned and unburned gas as suggested by Weinberg [1,2] and others. A practical requirement of such an exchanger is a minimal loss of heat to the surroundings. The analysis of one such device for heat exchange with reduced losses is the objective of the work reported herein. Fig. 1 illustrates the concept of heat recirculation in terms of enthalpy change along the coordinate of flow in a combustor. For normal combustion without preheating, the enthalpy change is indicated by the dashed line. Due to the existence of finite heat losses, the temperature does not attain the value for an adiabatic flame. On the other hand, enthalpy variation for preheating of the air or fuel by heat recirculation is represented by the solid line. Preheating air or fuel raises upstream enthalpy, and thereby produces an excess enthalpy flame whose temperature is higher than that of an adiabatic flame. By such means a very low heating value gas may be burned.

In this study, we first constructed an experimental five-pass burner of the heat-recirculating-type which combines a four-pass heat exchanger with a one-pass combustor. The heat exchanger preheats the air by recirculating some of the heat of combustion. The temperature of the preheated air and the temperature distribution of the burned gas within the combustor were measured for steady methane–air combustion, and the fundamental operating characteristics of the burner were determined as the equivalence ratio was varied within the fuel-lean regime.

Secondly, following the lead of the research by Churchill and Tepper [3], we set up a simple model for the process and solved it numerically to evaluate the temperature distributions of the air and burned gas throughout. In the calculations, the dependence not only on the equivalence ratio (a chemical parameter), but also on the Reynolds number,  $Re$  (a fluid–mechanical parameter), on the aspect ratio and the number of passes (geometrical parameters), was examined.

Thirdly, by comparing the results of the experimental measurements and the numerical simulations, we determined the influence of the various parameters on the characteristics of the burner. Since our primary interest is in optimization of the design of the burner from the viewpoint of heat recirculation, we expressed the fractional heat recirculation rate, which is defined as the ratio of the enthalpy

---

\*Corresponding author. Fax: +1-215-573-2093.

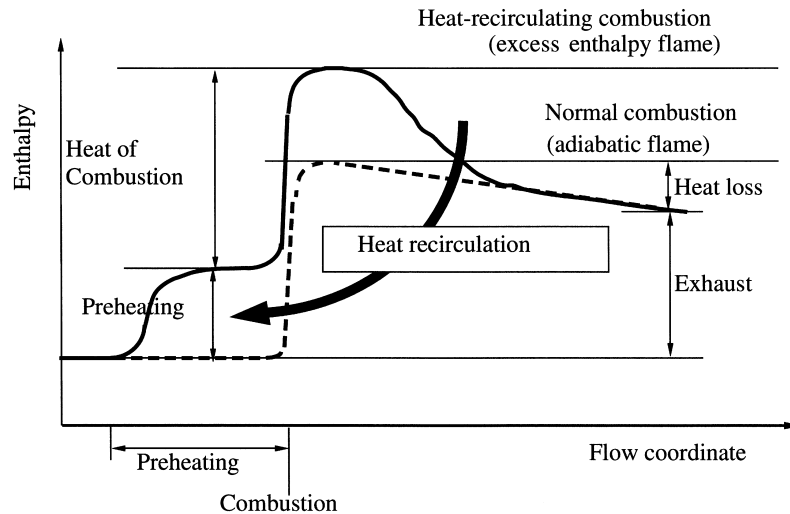


Fig. 1. Concept of heat recirculation.

increase by preheating air to the total heat of combustion, as a function of these several parameters.

## 2. Experimental measurements

Fig. 2 shows a vertical section of the experimental heat-recirculating burner. The device has a cylindrical shape with a height of 150 mm and a diameter of 60 mm, and is made of ceramic materials (ingredient:  $2\text{MgO}\cdot 2\text{Al}_2\text{O}_3\cdot 5\text{SiO}_2$ , thermal conductivity:  $\lambda = 1.8\text{--}3.5 \text{ W/m}\cdot\text{K}$ ). It is set on a stainless steel fuel injector with an inner diameter of 9 mm. In order to reduce heat losses, the overall burner is covered with thermal insulation with a thickness of 12.5 mm and a thermal conductivity of  $\lambda = 0.035 \text{ W/m}\cdot\text{K}$ .

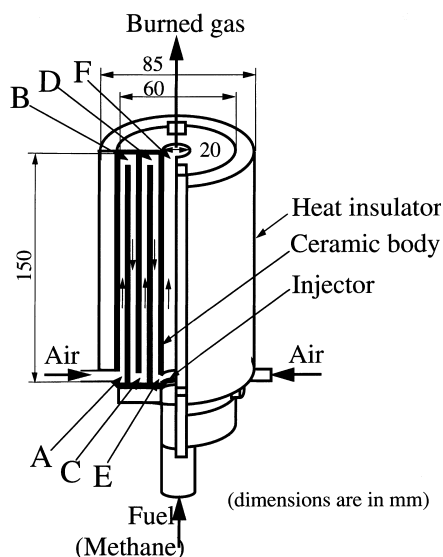


Fig. 2. A vertical section of a ceramic burner (4-pass heat exchanger + 1-pass combustor).

The burner consists of five coaxial passes in which the central one is a combustor and the outer four constitute an heat exchanger to preheat air with some of the heat of combustion. Room temperature air enters the first pass (the outermost one) at point A, and is gradually preheated by going up and down the first, second, third and fourth coaxial passes,  $A \rightarrow B$ ,  $B \rightarrow C$ ,  $C \rightarrow D$ ,  $D \rightarrow E$ . The preheated air is then mixed with room temperature methane introduced through the injector. Burning occurs at the inlet of the final pass (the central one),  $E'$ , as a result of forced ignition. A methane–air diffusion flame is then formed downstream of the injector. Finally the high temperature burned gas is exhausted from the outlet, F, through the final pass with a diameter of 20 mm,  $E' \rightarrow F$ .

The volumetric rates of air and methane were controlled by mass flow meters ahead of their inlets, keeping the total volumetric rate constant at  $Q = 14 \text{ l/min} = 7/30\,000 \text{ m}^3/\text{s}$ . The temperatures were measured with R-type thermocouples with a diameter of 0.1 mm at point E (preheated air temperature) and along the final pass  $E' \rightarrow F$  (burned gas temperature) without correction for radiation etc. These volumetric rates and uncorrected temperatures were simultaneously fed into a computer system to be recorded.

## 3. Numerical simulations

In the simple model used for computations, the following assumptions are made: (i) The air and burned gas flows are laminar since the equivalent  $Re$  is about 200, but they are treated as one-dimensional in the sense that the air and burned gas temperatures are postulated to be functions only of the vertical distance  $x$ ; (ii) heat transfer in a cross-section of the burner is considered to be dominant over that in the vertical direction; (iii) heat exchange due to radiation and heat losses from the upper and lower walls of the burner are ignored; (iv) the characteristic time of the chemical

reactions is postulated to be much smaller than that of the gas flow, i.e. the Damköhler number (the ratio of the time-scale for flow to that of reaction) is very large, and therefore mixing and combustion are completed at point E'.

Considering the energy balance of flow in each individual pass under the above assumptions, the air and burned gas temperatures along the  $x$ -direction of the  $i$ th pass,  $T_i(x)$  ( $i = 1, 2, 3, 4, 5$ ), are described by the following differential equations:

$$wc \frac{dT}{dx} = 2\pi a_2 U_2 (T_2 - T_1) + 2\pi a_1 U_1 (T_0 - T_1), \quad (1)$$

$$-wc \frac{dT_2}{dx} = 2\pi a_3 U_3 (T_3 - T_2) + 2\pi a_2 U_2 (T_1 - T_2), \quad (2)$$

$$wc \frac{dT_3}{dx} = 2\pi a_4 U_4 (T_4 - T_3) + 2\pi a_3 U_3 (T_2 - T_3), \quad (3)$$

$$-wc \frac{dT_4}{dx} = 2\pi a_5 U_5 (T_5 - T_4) + 2\pi a_4 U_4 (T_3 - T_4), \quad (4)$$

$$w'c' \frac{dT_5}{dx} = 2\pi a_5 U_5 (T_4 - T_5) \quad (5)$$

The boundary conditions on the upper and lower walls of the burner are, respectively,

$$T_1 = T_0, T_3 = T_2, T_5 = \frac{wc}{w'c'} T_4 + \Delta T \quad \text{at } x = 0, \quad (6)$$

and

$$T_2 = T_1, T_4 = T_3 \quad \text{at } x = 1 \quad (7)$$

Here  $w$  and  $w'$  are the mass rates of flows of air and burned gas,  $c$  and  $c'$  are the specific heat capacities at constant pressure of air and burned gas,  $a_i$  is the outer radius of the  $i$ th pass and  $U_i$  is the overall heat transfer coefficient based on the  $i$ th radius.  $T_0 = 298$  K is the room temperature of air and methane at the inlet of burner, and  $\Delta T$  is the temperature rise due to combustion. The chemico-thermodynamic properties, e.g. the adiabatic flame temperature and the final product composition, were solved by using a program for chemical equilibrium calculations.

The varying value of the overall heat transfer coefficient  $U_i$ , which characterizes heat transfer from the  $(i-1)$ th pass flow to the  $i$ th pass flow through the ceramic wall, is an important parameter of this model. It is given by

$$\frac{1}{a_i U_i} = \frac{1}{a'_{i-1} h_{i-1}} + \ln \left( \frac{a'_{i-1}}{a_i} \right) \frac{1}{\lambda} + \frac{1}{a_i h_i}, \quad (8)$$

where  $a_i$  and  $a'_i$  are the outer and inner radii of the  $i$ th pass,  $h_i$  is the convective heat transfer coefficient for the  $i$ th pass flow and  $\lambda$  is the thermal conductivity of the ceramic wall: The right hand of Eq. (8) includes both convection (the first and third terms) and thermal conduction (the second term) but not radiation. For the overall heat transfer coefficient of the outermost pass  $U_1$ , a term representing thermal conduction through thermal insulation with thermal conductivity  $\lambda_0$  is added. Since the temperature dependence of the

specific heat capacities and various transport coefficients is considered, the set of differential equations Eqs. (1)–(5) is non-linear in general and the interactive effects of gas flow and heat transfer are introduced by means of  $U_i$ .

#### 4. Non-dimensional parameters

Inlet and outlet temperatures, the surface area of the heat exchanger and factor accounting for economics may be identified as influential characteristics of the burner. In this study, as seen in Fig. 3, we are concerned with the influence of the following four parameters.

First, the chemical parameter, i.e. the equivalence ratio  $\phi$ , is defined as the ratio of methane-to-air divided by their stoichiometric ratio. Since our interest is limited to fuel-lean combustion, only the range of  $0 \leq \phi \leq 1$  is covered. The normal, stable, lower limit of flammability without preheating or heat recirculation is  $\phi = 0.56$  for a methane-air premixed flame.

Second, the fluid-mechanical parameter, i.e. the Re at the outlet, is defined as  $Re = ud/\nu$  where  $u = Q/\pi(d/2)^2$  is the velocity of the burned gas,  $\nu$  is the kinematic viscosity and  $d$  is the diameter of the central pass (the combustor). In practice, the upper limit of  $Re(Q)$  is imposed either by blow-off of the flame or by the onset of turbulence. Accordingly, the calculations were limited to  $Re < 1800$ .

Third and fourth, the aspect ratio  $l/d$  and the number of passes of the heat exchanger  $N$  are introduced as geometrical parameters of the burner. The former is defined as the ratio of the central pass length (the combustor length) to its diameter. The latter is increased by equal increments of spacing.

In the model, the temperature rise due to combustion  $\Delta T$  depends effectively on  $\phi$  alone since the thermal effects of incomplete combustion are known from chemical kinetic computations to be negligible for such lean flames and relatively long residence times at high temperature. The convective heat transfer coefficient  $h_i$  is estimated from the Nusselt number, Nu (the ratio of convection to conduction)

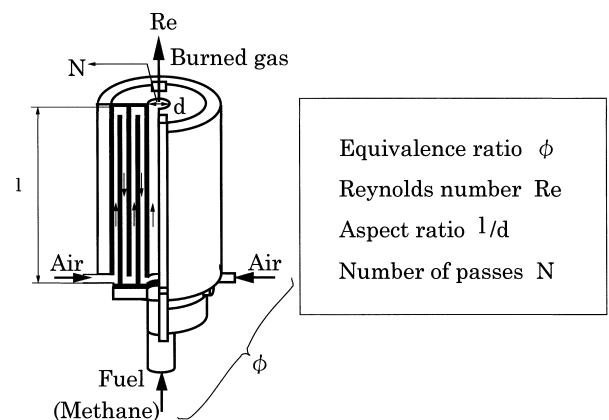


Fig. 3. Non-dimensional parameters.

which is in turn calculated from an empirical formula for laminar forced convection in a round tube as a function of the Reynolds number  $Re$ , the Prandtl number  $Pr$  and the aspect ratio  $l/d$ , i.e.  $Nu(Re, Pr, l/d)$ . Since  $Pr$  is determined by the physical properties of the gas,  $Nu$  varies only with  $Re$  and  $l/d$ . The heat exchange area of the burner increases as  $l/d$  and  $N$  increase, and the heat exchange time of the flowing gases increases as  $Re$  decreases or as  $l/d$  and  $N$  increase.

In the experiments, only the equivalence ratio was changed, leaving the other parameters fixed. On the other hand, in the calculations, the influence of all four parameters was examined. The two parameters related to the geometrical similarity of the burner are particularly difficult to change experimentally. Thus numerical simulations play an important role in generalizing the results.

## 5. Results and discussion

Fig. 4 illustrates the air and burned gas temperature distributions along the vertical axis of the burner. The curves represent the results from solving the model; the symbols (●) represent the experimental measurements, and (○) the theoretically calculated adiabatic flame temperatures. The conditions for the calculations were  $Re = 180$ ,  $l/d = 7.5$ ,  $N = 5$ ,  $\phi = 0.35, 0.25, 0.15$ , and  $0.07$ , the same as the experimental conditions. Room temperature air at point A is gradually preheated by going up and down the first, second, third and fourth passes,  $A \rightarrow B$ ,  $B \rightarrow C$ ,  $C \rightarrow D$ ,  $D \rightarrow E$ . The preheated air is then mixed with room temperature methane, and they burn at point E'. High-temperature burned gas is exhausted at F. In the experiments, the temperatures were measured at point E (preheated air temperature) and along the pass  $E' \rightarrow F$  (burned gas temperature). The computed profiles of burned gas temperature along the final pass,  $E' \rightarrow F$ , agree within 100 K with those of the experiments. As may be noted, most of the temperature rise in the preheated air takes place in the fourth pass,  $D \rightarrow E$ . The other passes,  $A \rightarrow B$ ,  $B \rightarrow C$ ,  $C \rightarrow D$ , appear to contribute very little, but that small contribution may be critical under some circumstances.

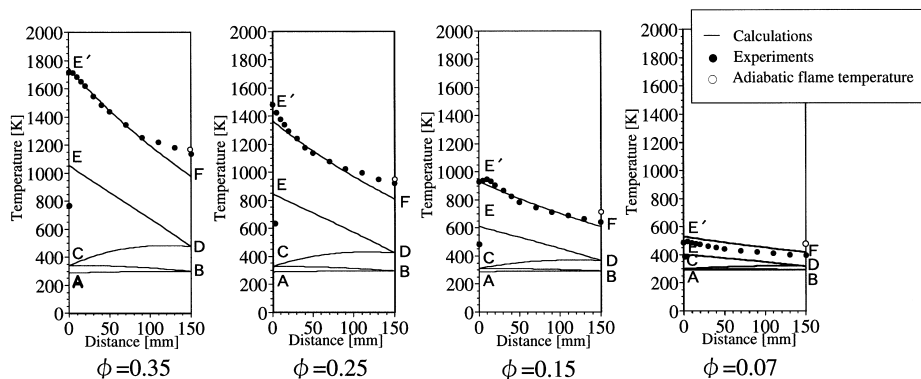


Fig. 4. Temperature distributions of air and burned-gas along the vertical axis of burner ( $Re = 180$ ,  $l/d = 7.5$ ,  $N = 5$ ).

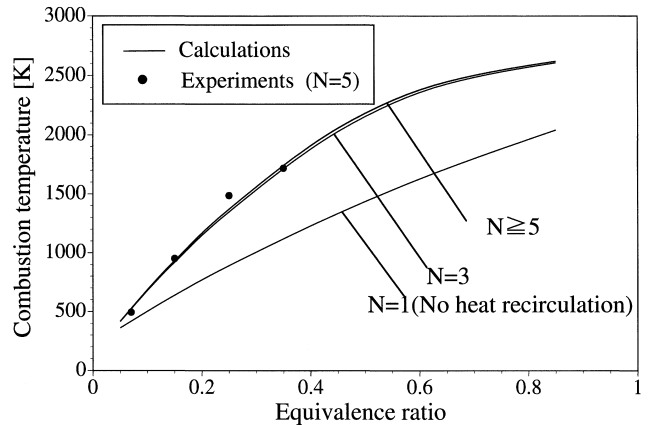


Fig. 5. Dependence of combustion temperature on equivalence ratio ( $Re = 180$ ,  $l/d = 7.5$ ).

The combustion temperature at point E' and the preheated air temperature at point E, as picked up from Fig. 4, and are included in Figs. 5 and 6, respectively. Experimental measurements were carried out for a five-pass burner ( $N = 5$ ) only, but the numerical simulations are for one, three, five, seven and an infinite number of passes ( $N = 1, 3, 5, 7, \infty$ ). The one-pass burner corresponds to a burner without heat exchange. As seen in Fig. 5, the cases of  $N \geq 3$  with heat recirculation (air preheating) result in excess enthalpy flames whose temperatures are about 100–700 K higher than that of the adiabatic flame. This allows stable combustion even in the regime below the normal flammability limit of  $\phi = 0.56$  for a normal methane–air premixed flame. Although the calculated results for the combustion temperature in Fig. 5 agree fairly well with experimental values, the calculated values of the preheated air temperature in Fig. 6 are about 200 K higher than the measured values. This disagreement is probably due to unaccounted heat losses in the modeling as well as to experimental inaccuracies.

Since the preheated air temperature is the most important factor characterizing the performance of the burner, it is necessary to determine this value as accurately as possible.

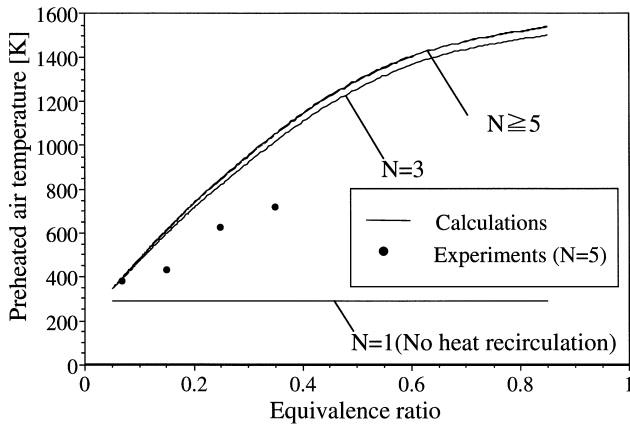


Fig. 6. Dependence of preheated air temperature on equivalence ratio (Re = 180, l/d = 7.5).

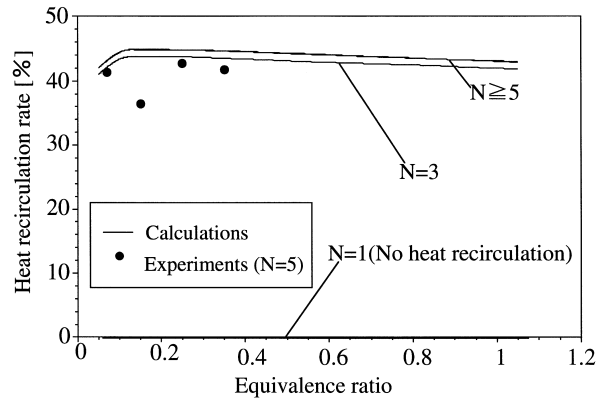


Fig. 8. Dependence of heat recirculation rate on equivalence ratio (Re = 180, l/d = 7.5).

Temperature itself is, however, not a completely satisfactory index for the effect of heat recirculation. A better criterion is the fractional heat recirculation rate, which is defined as the ratio of the enthalpy increase due to air preheating to that due to combustion. Using the enthalpy shown in Fig. 7, the fractional heat recirculation rate is represented by the ratio of B : A, while thermal efficiency is represented by the ratio of C : A. In the following discussion, we use the fractional heat recirculation rate as an index to characterize the heat transfer performance of the burner, and to examine dependence on various parameters.

Fig. 8 shows the dependence of the fractional heat recirculation rate on the equivalence ratio  $\phi$  for Re = 180 and l/d = 7.5. As  $\phi$  changes, the rate remains constant whereas the preheated air temperature increases in proportion to  $\phi$ . The fractional heat recirculation rate is estimated to be 0.44 from the calculations and to be 0.42 from the experiments. Improved performance due to increasing N is hardly evident. Since no heat recirculation (air preheating) is

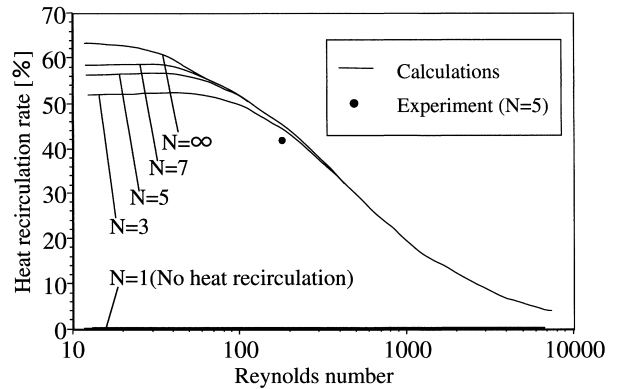


Fig. 9. Dependence of heat recirculation rate on Re ( $\phi = 0.25$ , l/d = 7.5).

performed in a one-pass burner (N = 1), the fractional rate of heat recirculation is zero.

Fig. 9 shows the dependence of the fractional heat recirculation rate on the Re at the outlet for  $\phi = 0.25$  and l/d = 7.5. As Re decreases, i.e. as the total volumetric rate of gas flow and the velocity decrease, the heat exchange time of the flowing gas increases and the fractional heat recirculation rate also increases. Particularly, in the regime of  $Re \leq 100$ , it becomes possible to obtain fractional heat recirculation rates greater than 0.50. As N increases, the rate also rises in the regime of very small Re. However, such an improvement is only about 10% at most, so only a few passes can be justified in practice.

Finally, Fig. 10 shows the dependence of the fractional heat recirculation rate on the aspect ratio l/d for  $\phi = 0.25$  and Re = 180. As l/d increases, the fractional heat recirculation rate also increases, and the rate seems to approach a constant value for  $l/d \geq 20$ . However, the increase of l/d is accompanied by an increase in the surface area of the burner, and increased heat losses. The result is a drop in the thermal efficiency of the burner. Therefore, these parameters must be controlled appropriately while keeping the thermal efficiency high.

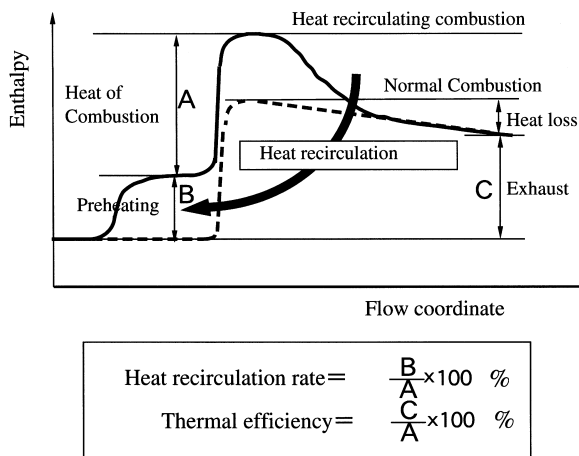


Fig. 7. Heat recirculation rate and thermal efficiency.

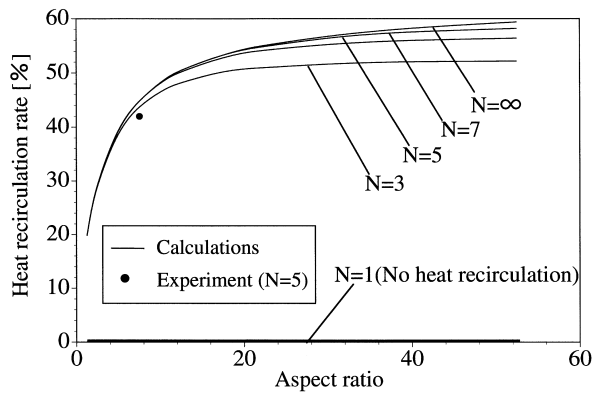


Fig. 10. Dependence of heat recirculation rate on aspect ratio ( $Re = 180$ ,  $\phi = 0.25$ ).

## 6. Conclusions

An experimental burner of the heat-recirculating-type was constructed and its thermal characteristics were investigated for methane–air fuel-lean combustion. Experimental measurements and numerical simulations of temperature distributions of air and burned gas flowing in the passes of the burner agreed reasonably well.

Using the fractional heat recirculation rate as a criterion for the characteristics of the burner, the optimal design of the burner was discussed. In particular, we examined the influences of a chemical parameter (the equivalence ratio), a fluid–mechanical parameter (the Reynolds number) and two geometrical parameters (the aspect ratio and the number of passes). The fractional heat recirculation rate is almost constant as the equivalence ratio varies, but it depends on the  $Re$  and the aspect ratio. Since the fractional heat recirculation rate increases only slightly with the number of passes, only a few passes are needed in practice. The measurements and computations provide valuable insights for the design of heat-recirculating exchangers even for other applications.

## References

- [1] F.J. Weinberg, *Nature* 233 (1971) 239–241.
- [2] S.A. Lloyd, F.J. Weinberg, *Nature* 251 (1974) 47–49.
- [3] S.W. Churchill, P. Tepper, *Ind. Eng. Chem. Process Des. Dev.* 24 (1985) 542–550.